MIT Open Access Articles

Rigid-Plastic Approximations for Predicting Plastic Deformation of Cylindrical Shells Subject to Dynamic Loading

Massachusetts Institute of Technology

Michelle S. Hoo Fatt

Tomasz Wierzbicki

*Department of Ocean Engineering
Massachusetts Institute of
Technology
Cambridge, MA 02139*

Minos Moussouros

John Koenig

*Naval Surface Warefare Center
Indian Head Division
Silver Spring, MD*

Rigid-Plastic Approximations for Predicting Plastic Deformation of Cylindrical Shells Subject to Dynamic Loading

A theoretical approach was developed for predicting the plastic deformation of a cylindrical shell subject to asymmetric dynamic loads. The plastic deformation of the leading generator of the shell is found by solving for the transverse deflections of a rigid-plastic beam/string-on-foundation. The axial bending moment and tensile force in the beam/string are equivalent to the longitudinal bending moments and membrane forces of the shell, while the plastic foundation force is equivalent to the shell circumferential bending moment and membrane resistances. Closed-form solutions for the transient and final deformation profile of an impulsive loaded shell when it is in a "string" state were derived using the eigenfunction expansion method. These results were compared to DYNA 3D predictions. The analytical predictions of the transient shell and final centerline deflections were within 25% of the DYNA 3D results. © 1996 John Wiley & Sons, Inc.

INTRODUCTION

The objective of this study is to develop a general approach for predicting the plastic deformation of a cylindrical shell subject to dynamic loading. The shell is subject to a "side-on" pressure load (i.e., one in which the loading is asymmetric in the circumferential direction). Previous analytical attempts by Witmer et al. (1960) and Greenspon (1970) to solve this problem resulted in closed-form expressions for the final deformation and response time of the shell, but these solutions do not give the transient deformation of the shell. Several commercially available numerical codes (see for example, Underwood, 1972; Stricklin et al., 1974; Jiang and Olson, 1991) are also available

for finding the transient deformation of the shell, and the analytical model will be compared with DYNA 3D numerical predictions produced by Moussouros and Koenig (1994). The particular example chosen for comparing the analytical solution with DYNA 3D predictions is an aluminum shell subjected to asymmetric impulsive loading.

It is well known that the coupled nonlinear partial differential equations that govern shell deformation are mathematically intractable if the loading to the shell is asymmetric because derivatives with respect to the circumferential direction must be retained. In the following theory, the distribution of the shell deformation in the circumferential direction is specified by considering a kinematically admissible plastic collapse mech-

anism of a ring in plane strain. The circumferential distribution of the ring deformation is assumed to be the same for each cross section of the shell, and the function used to describe it yields "equivalent functions," i.e., average values of shell quantities found by integration with respect to the circumferential coordinate. It will be shown subsequently that by deriving equivalent shell functions, one may represent the longitudinal bending moment and membrane force of the shell as the axial bending moment and tensile force in a beam/string, and the circumferential bending moment and membrane compression as a plastic foundation that supports the beam/string. The equivalent functions are functions only of axial direction, and thus enable us to solve the two-dimensional (2-D) shell as a 1-D beam/string-on-foundation. The beam-on-foundation model for the shell has been used to model shells undergoing large plastic deformation and gave useful results in applications such as the pinching of tubes (Reid, 1978), the denting of tubes (Wierzbicki and Suh, 1988), and projectile impact into thin cylindrical shells (Yu and Stronge, 1990).

In developing the theoretical model for the shell, we assume a material that is isotropic, rate independent, and rigid-plastic. A general methodology for reducing the 2-D shell problem subjected to dynamic pressure loads into a 1-D problem involving a rigid-plastic beam/string resting on a rigid-plastic foundation and subjected to equivalent line load is first derived in this article. This is then followed by the solution for a special case of an impulsively loaded shell using the eigenfunction expansion method. Finally, the analytical solutions for the transient and final deformation of the impulsively loaded shell are compared to DYNA 3D predictions.

THEORETICAL FORMULATION

Consider a long cylindrical shell of thickness n and radius R as shown in Fig. 1. The cylinder is subjected to an inward radial pressure pulse $p(x, \theta, t)$ only on the upper half of the cylinder. The load is asymmetric, but it has two planes of symmetry at $x = 0$ and $\theta = 0$. The load intensity is such that the shell experiences localized plastic deformation, i.e., the maximum extent in the hoop direction is of the order of the shell radius or smaller, and the axial distribution of the shell deformation spans over a few shell radii. In addition to the inward radial pressure are radial shear

force F_r, axial force F_x, and bending moment T at the ends of the shell.

As a result of these loads, the shell undergoes deformation $\mathbf{u}(x, \theta, t)$, where x, θ denotes the axial and circumferential coordinates and t denotes time, and rigid body displacement in the radial direction $w|_{end}$ and axial direction $u|_{end}$, and rotation $w'|_{end}$ at the ends.

Material Idealization

In the theoretical formulation of the problem, the material is assumed to be isotropic, time-independent, and rigid-plastic. Neglect of elasticity and strain rate tends to increase the value of the flow stress σ_o of most ductile materials, and the rigid-plastic approximation provides an upper bound for shell deformations.

Material strain hardening may be taken into account by using the concept of an average flow stress σ_o, which lies somewhere between the yield and ultimate strength. (The flow strength is calculated by requiring equal areas under the actual material stress–strain curve and the approximate rigid-plastic stress–strain curve.) When the material undergoes considerable work hardening, the flow stress represents a constant, elevated stress corresponding to an average strain ε_{av} during the loading process, $\sigma_o = \sigma(\varepsilon_{av})$. An average strain during the loading process is then evaluated from the solution for the deformation based on the assumed flow stress. If the calculated average strain corresponds to the assumed flow stress, then the rigid-plastic solution is consistent with the assumed flow stress. If both are not consistent with each other, the flow stress that corresponds to the average strain is evaluated and used to derive a new solution for shell deformation. The iterative process is repeated until the average strain and flow stress are in agreement with the material stress–strain relation.

Dynamic Equilibrium

The overall shell equilibrium is expressed via the principle of virtual velocities

$$\dot{D} \equiv \int_V \sigma_{ij}\dot{\varepsilon}_{ij}\, dV = \int_S \mathbf{p}\dot{\mathbf{w}}\, dS - \int_V \rho\ddot{\mathbf{w}}\dot{\mathbf{w}}\, dV, \quad (1)$$

where ($\dot{\ }$) denotes $\partial/\partial t$, $\dot{D}$ is the rate of plastic work dissipated, σ_{ij} and $\dot{\varepsilon}_{ij}$ denote stress and
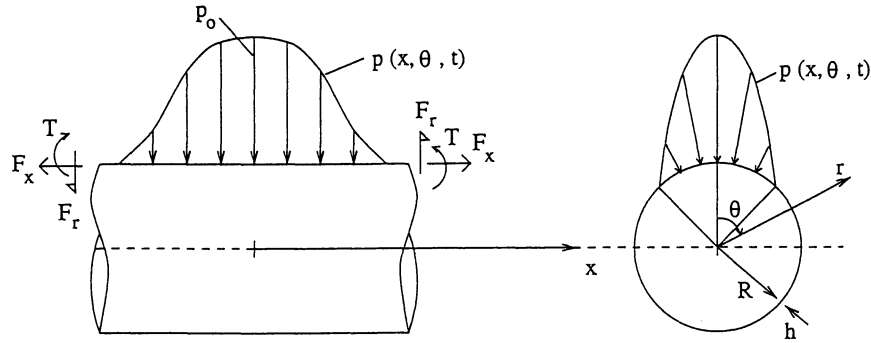
FIGURE 1 Geometry of and loading on the cylindrical shell.

strain rate, **w** is the displacement vector, and **p** is a generalized surface traction.

In shell coordinates for which a differential shell element is $dS = dx\, R\, d\theta$, the above equation is expressed as

$$2 \int_0^\xi 2R \int_0^\pi (M_{\alpha\beta} \dot{\kappa}_{\alpha\beta} + N_{\alpha\beta} \dot{\varepsilon}_{\alpha\beta})\, d\theta\, dx$$

$$= 2 \int_0^\xi 2R \int_0^\pi p_o \dot{w}\, d\theta\, dx + 2 \cdot 2R \int_0^\pi F_x \dot{u}|_{end}\, d\theta$$

$$+ 2 \cdot 2R \int_0^\pi F_r \dot{w}|_{end}\, d\theta + 2 \cdot 2R \int_0^\pi T\dot{w}'|_{end}\, d\theta$$

$$- 2 \int_0^\xi 2R \int_0^\pi m(\ddot{u}\dot{u} + \ddot{v}\dot{v} + \ddot{w}\dot{w}')\, d\theta\, dx, \quad (2)$$

where ξ is the extent of plastic deformation, $[\alpha, \beta] = [x, \theta]$; $M_{\alpha\beta}$ and $N_{\alpha\beta}$ are the corresponding tensors of the bending moment and membrane force; $\dot{\kappa}_{\alpha\beta}$ and $\dot{\varepsilon}_{\alpha\beta}$ are curvature and strain rates; the velocity vector $\dot{\mathbf{w}}[\dot{u}, \dot{v}, \dot{w}]$ corresponds to the x, θ, r axis; **p** is a vector of surface tractions with components $\mathbf{p}[0, 0, p_o]$ in the x, θ, r direction; and $m = \rho h$ is the mass per unit shell area.

The bending moments $M_{\alpha\beta}$ and membrane forces $N_{\alpha\beta}$ are coupled through a yield condition,

$$f(M_{\alpha\beta}, N_{\alpha\beta}) = 0, \quad (3)$$

which is assumed to be a plastic potential for the generalized strain rates

$$\dot{\kappa}_{\alpha\beta} = \lambda \frac{\partial f}{\partial M_{\alpha\beta}}, \quad \dot{\varepsilon}_{\alpha\beta} = \lambda \frac{\partial f}{\partial N_{\alpha\beta}}, \quad (4)$$

where λ is a proportionality constant.

An expression of the rate of plastic work dissipated in the shell $\dot{D}$ is

$$\dot{D} = 2 \int_0^\xi 2R \int_0^\pi (M_{xx} \dot{\kappa}_{xx} + M_{\theta\theta} \dot{\kappa}_{\theta\theta} + 2M_{x\theta} \dot{\kappa}_{x\theta}$$
$$+ N_{xx} \dot{\varepsilon}_{xx} + N_{\theta\theta} \dot{\varepsilon}_{\theta\theta} + 2N_{x\theta} \dot{\varepsilon}_{x\theta})\, d\theta\, dx. \quad (5)$$

Previous analyses by Wierzbicki and Suh (1988) and Moussouros and Hoo Fatt (1995) showed that the contribution of plastic work associated with shear deformation is 10–15% of the total plastic work dissipated in tubes subject to transverse "knife" loading. As a first-order approximation, assume that $M_{x\theta} \dot{\kappa}_{x\theta} = N_{x\theta} \dot{\varepsilon}_{x\theta} = 0$, so that the rate of plastic dissipation simplifies to

$$\dot{D} = 2 \int_0^\xi 2R \int_0^\pi (M_{xx} \dot{\kappa}_{xx} + M_{\theta\theta} \dot{\kappa}_{\theta\theta} + N_{xx} \dot{\varepsilon}_{xx}$$
$$+ N_{\theta\theta} \dot{\varepsilon}_{\theta\theta})\, d\theta\, dx. \quad (6)$$

Strain-Displacement Relations

If we confine our analysis to moderately large deflection and small strains, the Lagrangian description of the axial strain and curvature rates are (Brush and Almroth, 1975)

$$\dot{\varepsilon}_{xx} = \dot{u}' + w'\dot{w}', \quad (7)$$

$$\dot{\kappa}_{xx} = -\dot{w}'', \quad (8)$$

where $(\quad)'$ denotes $\partial/\partial x$.

Equivalent Functions

Substituting Eqs. (7) and (8) into Eq. (2) gives the following statement of dynamic equilibrium:

$$-2 \int_0^\xi 2R \int_0^\pi M_{xx} \dot{w}''\, d\theta\, dx$$

$$+ 2 \int_0^\xi 2R \int_0^\pi N_{xx}(\dot{u}' + w'\dot{w}')\, d\theta\, dx$$

$$+ 2 \int_0^\xi 2R \int_0^\pi (N_{\theta\theta} \dot{\varepsilon}_{\theta\theta} + M_{\theta\theta} \dot{\kappa}_{\theta\theta}) \, d\theta \, dx$$

$$= 2 \int_0^\xi 2R \int_0^\pi p_o \dot{w} \, d\theta \, dx + 2 \cdot 2R \int_0^\pi F_x \dot{u} \big|_{\text{end}} \, d\theta$$

$$+ 2 \cdot 2R \int_0^\pi F_r \dot{w} \big|_{\text{end}} \, d\theta + 2 \cdot 2R \int_0^\pi T \dot{w}' \big|_{\text{end}} \, d\theta$$

$$- 2 \int_0^\xi 2R \int_0^\pi m(\ddot{u}\dot{u} + \ddot{v}\dot{v} + \ddot{w}\dot{w}) \, d\theta \, dx. \tag{9}$$

Assume: tangential deformations are negligible, i.e., $v = 0$; there is no warping, i.e., u is independent of θ; and cross-sections of the deforming shell are similar and correspond to a plastically deforming ring in plane strain whose deformation field may be described in terms of its centerline deflection $w(x, \theta = 0, t) = w_o(x, t)$. For a given deformation field, each term in Eq. (9) may be integrated with respect to the circumferential coordinate to give the following expression for deriving equivalent functions: an equivalent line load,

$$\bar{p}(x, t) \cdot \dot{w}_o = 2R \int_0^\pi p_o \dot{w}(x, \theta, t) \, d\theta, \tag{10}$$

an equivalent mass per unit length,

$$\bar{m}(x, t) \cdot \ddot{w}_o \dot{w}_o = 2Rm \int_0^\pi \ddot{w}\dot{w}(x, \theta, t) \, d\theta, \tag{11}$$

an equivalent ring crushing resistance,

$$\bar{q}(x, t) \cdot \dot{w}_o = 2R \int_0^\pi (M_{\theta\theta} \dot{\kappa}_{\theta\theta} \\ + N_{\theta\theta} \dot{\varepsilon}_{\theta\theta})(x, \theta, t) \, d\theta, \tag{12}$$

an equivalent axial bending moment,

$$\bar{M}(x, t) \cdot \dot{w}_o'' = 2R \int_0^\pi M_{xx} \dot{w}''(x, \theta, t) \, d\theta, \tag{13}$$

an equivalent axial membrane force,

$$\bar{N}(x, t) \cdot w_o' \dot{w}_o' = 2R \int_0^\pi N_{xx} w' \dot{w}'(x, \theta, t) \, d\theta, \tag{14}$$

an equivalent applied axial force,

$$\bar{F}_x \cdot \dot{u}_o \big|_{\text{end}} = 2R \int_0^\pi F_x \dot{u} \big|_{\text{end}} \, d\theta, \tag{15}$$

an equivalent applied shear force,

$$\bar{F}_r \cdot \dot{w}_o \big|_{\text{end}} = 2R \int_0^\pi F_r \dot{w} \big|_{\text{end}} \, d\theta, \tag{16}$$

an equivalent applied bending moment,

$$\bar{T} \cdot \dot{w}_o' \big|_{\text{end}} = 2R \int_0^\pi T \dot{w}' \big|_{\text{end}} \, d\theta. \tag{17}$$

All equivalent functions depend on variables x and t; they are a consequence of the dynamic response of the shell. Even the equivalent mass varies with position and time because of varying inertia forces induced by the shell motion.

Introducing equivalent functions into Eq. (9) gives

$$2 \int_0^\xi [-\bar{M}\dot{w}_o'' + \bar{q}\dot{w}_o + 2\pi R N_{xx} \dot{u}_o' + \bar{N}w_o'\dot{w}_o'] \, dx$$

$$= 2\bar{F}_x \dot{u}_o \big|_{\text{end}} + 2\bar{F}_r \dot{w}_o \big|_{\text{end}} + 2\bar{T}\dot{w}_o' \big|_{\text{end}}$$

$$+ 2 \int_0^\xi \bar{p}\dot{w}_o \, dx \tag{18}$$

$$- 2 \int_0^\xi [2\pi R m \ddot{u}_o \dot{u}_o + \bar{m}\ddot{w}_o\dot{w}_o] \, dx.$$

Integrating Eq. (18) by parts, one gets

$$(\bar{N}w' - \bar{M}' - \bar{F}_r)\dot{w}_o \big|_{\text{ends}} + \int_0^\xi [\bar{m}\ddot{w}_o + \bar{M}''$$

$$- (\bar{N}w_o')' + \bar{q} - \bar{p}]\dot{w}_o \, dx + (2\pi R N_{xx} - \bar{F}_x)\dot{u}_o \big|_{\text{ends}}$$

$$+ \int_0^\xi 2R\pi(-N_{xx}' + m\ddot{u}_o)\dot{u}_o \, dx + (\bar{M} - \bar{T})\dot{w}_o' \big|_{\text{ends}} = 0 \tag{19}$$

The above equations are valid for all virtual velocities. Therefore,

$$\bar{m}\ddot{w}_o + \bar{M}'' - (\bar{N}w_o')' + \bar{q} = \bar{p} \tag{20}$$

with boundary conditions $\bar{N}w' - \bar{M}' = \bar{F}_r$ or $\dot{w}_o \big|_{\text{end}} = 0$ and $\bar{M} = \bar{T}$ or $\dot{w}_o' \big|_{\text{end}} = 0$, and

$$m\ddot{u}_o - N_{xx}' = 0 \tag{21}$$

with boundary condition $2\pi R N_{xx} = \bar{F}_x$ or $\dot{u}_o \big|_{\text{end}} = 0$.

Equations (20) and (21) describe the equations of motion in the radial direction of the leading generator ($\theta = 0$) and axial directions, respectively. Each equation is subjected to either force or displacement boundary conditions; i.e., moments and equivalent shear forces or slopes and radial deflections are specified in Eq. (20), while

axial forces or axial displacements are specified in Eq. (21).

Impulsive Loading

In elasticity, the pressure loading can be expressed as an impulsive loading if the pulse duration of the pressure load impinging on the shell is much less than the fundamental period of vibration of the shell. In plasticity, the pressure loading is considered as an impulsive loading if the pulse duration is much shorter than the response time of the shell. (Vibrations do not occur because plastic work is dissipated instead of being stored as in an elastic body.) The magnitude and distribution of the initial velocity of the shell is governed by the impulse intensity, the shell impedance (ρh), and the shell geometry, outer radius, and length.

To find the corresponding impulsive loading $I(x, \theta)$, the pressure pulse is integrated in time and the loading to the shell is introduced as an initial shell velocity $V_o(x, \theta)$. The magnitude of the initial velocity is calculated from the transfer of linear momentum to the shell,

$$\int_0^\infty p(x, \theta, t) \, dt = I(x, \theta) = mV_o(x, \theta), \quad (22)$$

where I is the specific impulse with units *pressure time* (not to be confused with an impulse with units force time) and $m = \rho h$ is the mass per unit area or material impedance.

An equivalent impulse load $\bar{I}$ is then given by

$$\bar{I}(x) = \int_0^\infty 2R \int_0^\pi p(x, \theta, t) \dot{w}(x, \theta, t) \, d\theta \, dt$$
$$= \overline{m}\overline{V}_o(x). \quad (23)$$

Neglect of Axial Deformation

If we confine our analysis to a plastic foundation with an infinite shear resistance but finite compressive resistance $\bar{q}$, $u \approx 0$ and consequently, $\dot{u} = \ddot{u} = 0$.

Setting $\ddot{u} = 0$ in Eq. (19) gives only an equation of motion for the radial deflection of the leading generator

$$\overline{m}\ddot{w}_o + \overline{M}'' - (\overline{N}w_o')' + \bar{q} = \bar{p}, \quad (24)$$

with boundary conditions $\overline{N}w_o' - \overline{M}' = \overline{F}_r$ and $\overline{M} = \overline{T}$.

The above equation of motion is recognized as the rigid-plastic beam equation with finite deflections. No rigorous theoretical methods have been proposed for solving finite deflections of a rigid-plastic beam. Several approximate solutions, which are in good agreement with experimental results, were proposed by Jones (1971) and Vaziri et al. (1987). Rigorous analytical solutions for limiting cases of Eq. (24) do exist and these will be explained below.

Beam-on-Foundation

When deflections are infinitesimal, the equivalent axial membrane force is negligible compared to the equivalent axial bending moment. Omitting the $(\overline{N}w_o')'$ term in Eq. (24) gives

$$\overline{m}\ddot{w}_o + \overline{M}'' + \bar{q} = \bar{p}, \quad (25)$$

subject to the boundary conditions $\overline{N}w_o' - \overline{M}' = \overline{F}_r$ and $\overline{M} = \overline{T}$. Yu and Stronge (1990) used the above equation to derive solutions for the transient deformation of cylinders subject to projectile impact. When shell deformations become large, they included a membrane factor to account for axial membrane forces in an approximate way.

String-on-Foundation

When the plastic deformation of an axially restained shell are finite, axial membrane forces can no longer be ignored. The axial bending moment dominates the shell response during infinitesimal deflection, but it becomes less significant when compared to the axial membrane force as the shell deflections increase. Haythornwaite (1961) demonstrated that a fully clamped rigid-plastic beam will enter a membrane state when the beam deflections are of the order of the thickness of the beam. A similar phenomenon is assumed to take place for the rigid-plastic shell. Neglecting the axial bending moment in Eq. (24) gives

$$\overline{m}\ddot{w}_o - (\overline{N}w_o')' + \bar{q} = \bar{p}, \quad (26)$$

subject to the boundary condition $\overline{N}w_o' = \overline{F}_r$. In the following sections, we present a solution for the cylinder in a purely membrane state and compare the analytical predictions to DYNA 3D results.

STRING-ON-FOUNDATION SUBJECT TO IMPULSIVE LOADING

As an example, consider a fully-clamped cylinder of finite length $2L$. The cylinder is subject to asymmetric impulsive loading. The circumferential distribution of the impulsive load is a cosine function on the upper half of the shell circumference. Two impulsive load distributions in the axial direction are considered, a parabolic distribution and a uniform distribution. The shell undergoes radial deformation $w(x, \theta, t)$, where x and θ denote the axial and circumferential coordinates and t denotes time.

Based on the string-on-foundation analogy for the shell, the equation for the plastic deformation of the leading generator of the shell ($\theta = 0$) under impulsive loading is

$$\overline{m}\ddot{w}_o - (\overline{N}w'_o)' + \overline{q} = 0. \tag{27}$$

The shell is clamped at both ends so that Eq. (27) is subject to the boundary conditions

$$w'_o = 0 \quad \text{at } x = 0 \tag{28}$$

and

$$w_o = 0 \quad \text{at } x = \pm L. \tag{29}$$

The initial-boundary partial differential equation is also subject to the initial conditions

$$w_o = 0 \quad \text{at } t = 0 \tag{30}$$

and

$$\dot{w}_o = \overline{V}_o(x) \quad \text{at } t = 0, \tag{31}$$

where $\overline{V}_o(x)$ is the initial velocity distribution along the length of the shell.

It is assumed for simplicity that equivalent functions are constant. The initial-boundary value problem can then be expressed in terms of the following normalized variables:

1. $\bar{x} = x/L$, axial coordinate
2. $\bar{t} = tc/L$, time
3. $\bar{w} = w_o\overline{N}/L^2\overline{q}$, transverse deflection

where $c = \sqrt{\overline{N}/\overline{m}}$ is the plastic wave speed in the string.

Denoting derivatives with respect to the normalized variables gives

$$\bar{w}_{\bar{t}\bar{t}} - \bar{w}_{\bar{x}\bar{x}} + 1 = 0, \tag{32}$$

with boundary conditions

$$\bar{w}_{\bar{x}} = 0 \quad \text{at } \bar{x} = 0 \tag{33}$$

and

$$\bar{w} = 0 \quad \text{at } \bar{x} = 1, \tag{34}$$

and initial condiions

$$\bar{w} = 0 \quad \text{at } \bar{t} = 0 \tag{35}$$

and

$$\bar{w}_{\bar{t}} = \bar{V}(\bar{x}) \quad \text{at } \bar{t} = 0, \tag{36}$$

where the normalized velocity is $\bar{V} = V_o\overline{N}/(cL\overline{q})$.

Eigenfunction Expansion

Reduce the problem into a homogeneous system of equations by assuming a solution of the form

$$\bar{w} = \Phi - \tfrac{1}{2}(1 - \bar{x}^2). \tag{37}$$

The homogeneous system is

$$\Phi_{\bar{t}\bar{t}} - \Phi_{\bar{x}\bar{x}} = 0, \tag{38}$$

with boundary conditions

$$\Phi_{\bar{x}} = 0 \quad \text{at } \bar{x} = 0 \tag{39}$$

and

$$\Phi = 0 \quad \text{at } \bar{x} = 1, \tag{40}$$

and initial conditions

$$\Phi = \tfrac{1}{2}(1 - \bar{x}^2) \quad \text{at } \bar{t} = 0 \tag{41}$$

and

$$\Phi_{\bar{t}} = \bar{I}f(\bar{x}) \quad \text{at } \bar{t} = 0, \tag{42}$$

where $\bar{I}$ is the amplitude of the dimensionless impulse and $f(\bar{x})$ is the axial distribution of the impulse.

Equation (39) is automatically satisfied if

$$\Phi = \sum_{n=1}^{\infty} [A_n \sin(\lambda_n\bar{t}) + B_n \cos(\lambda_n\bar{t})] \cos(\lambda_n\bar{x}). \tag{43}$$

The eigenvalues are determined from condition (40) so that

$$\cos \lambda_n = 0 \text{ or } \lambda_n = (2n - 1)\pi/2, \text{ for } n = 1, 2, 3, \ldots \quad (44)$$

The solution is thus

$$\bar{w} = \sum_{n=1}^{\infty} [A_n \sin(\lambda_n \bar{t}) + B_n \cos(\lambda_n \bar{t})] \cos(\lambda_n \bar{x}) \\ - \tfrac{1}{2}(1 - \bar{x}^2). \quad (45)$$

The eigenfunction coefficients are found from the initial conditions, Eqs. (41) and (42),

$$\sum_{n=1}^{\infty} B_n \cos(\lambda_n \bar{x}) = \tfrac{1}{2}(1 - \bar{x}^2) \quad (46)$$

and

$$\sum_{n=1}^{\infty} A_n \lambda_n \cos(\lambda_n \bar{x}) = \bar{I} f(\bar{x}). \quad (47)$$

The value of B_n is

$$B_n = \frac{2 \sin \lambda_n}{\lambda_n^3}. \quad (48)$$

The value of A_n depends on the axial distribution of the impulse, $f(\bar{x})$,

$$A_n = \begin{cases} \dfrac{4\bar{I} \sin \lambda_n}{\lambda_n^4}, & \text{if } f(\bar{x}) = 1 - \bar{x}^2 \\[2mm] \dfrac{2\bar{I} \sin \lambda_n}{\lambda_n^2}, & \text{if } f(\bar{x}) = 1. \end{cases} \quad (49)$$

Using $\tfrac{1}{2}(1 - \bar{x}^2) = \sum_{n=1}^{\infty} B_n \cos(\lambda_n \bar{x})$, we can also express Eq. (45) as

$$\bar{w} = \sum_{n=1}^{\infty} [A_n \sin(\lambda_n \bar{t}) + B_n[\cos(\lambda_n \bar{t}) - 1]] \cos(\lambda_n \bar{x}). \quad (50)$$

Unloading and Final Deformation

The generalized strain rates, i.e., strain rate and velocity rate, in the string-on-foundation model are $\bar{\varepsilon}_{\bar{t}}$, $\dot{\bar{w}}_{\bar{t}}$, where $\varepsilon_{\bar{t}} = \bar{w}_{\bar{x}} \bar{w}_{\bar{x}\bar{t}}$. The unloading condition is formulated in the space of the strain rate vector. One can distinguish two cases of partial unloading and full unloading. Partial unloading occurs when only one component of the generalized strain rate vanishes ($\bar{\varepsilon}_t = 0$, $\dot{\bar{w}}_{\bar{t}} \neq 0$ or $\dot{\bar{w}}_{\bar{t}} =$

0, $\bar{\varepsilon}_{\bar{t}} \neq 0$). Full unloading takes place when both components are zero.

An exact unloading analysis was performed by Suliciu et al. (1995) in a related problem of an infinite string on a plastic foundation loaded impulsively. Using the method of characteristics, several regions were identified in the phase plane $(\bar{x}, \bar{t})$. The analysis was complicated and involved propagation of rigid zones into an already deformed plastic string.

The present solution methodology, based on the eigenvalue expansion method, covers a fixed length of the beam and precludes the application of the rigorous unloading analysis. Instead, an approximate and more restrictive unloading criterion is proposed.

The solution in the loading region, Eq. (50), is expressed in terms of an infinite series of modal function $\cos(\lambda_n \bar{x})$ and variable coefficients $\bar{w}_n(\bar{t})$

$$\bar{w}(\bar{x}, \bar{t}) = \sum_{n=1}^{\infty} \bar{w}_n(\bar{t}) \cos(\lambda_n \bar{x}). \quad (51)$$

For impulsive loading with expansion coefficients specified by Eqs. (48) and (49), the amplitudes $\bar{w}_n(\bar{t})$ are diminishing functions of time. Each amplitude reaches a maximum value when the corresponding velocity vanishes

$$\dot{\bar{w}}_{\bar{t}}(\lambda_n, \bar{t}_n) = 0. \quad (52)$$

It can be shown that higher modes decay more rapidly than the lower ones. It is assumed that each mode contributes to the final deflection of the structure only in the time $0 < \bar{t} < \bar{t}_n$,

$$\bar{w}_n(\bar{t}) = \begin{cases} [A_n \sin(\lambda_n \bar{t}) + B_n[\cos(\lambda_n \bar{t}) - 1]], \\ \qquad\qquad \text{for } 0 < \bar{t} < \bar{t}_n \\ 0 \qquad\qquad \text{for } \bar{t} > \bar{t}_n, \end{cases} \quad (53)$$

where $\bar{t}_n$ is defined by Eq. (52).

According to the above criterion, all modes contributes to the shell response early on. Later only the lower modes survive and the motion ends with the fundamental mode. This criterion of progressive switching off of higher modes has many advantages. It confirms the property of mode convergence proven by Martin and Symonds (1966) for general rigid, perfectly plastic structures. It also leads to a much desired closed-form solution for the final deflection, giving realistic permanent shapes of the deformed shell. Fi-

nally, it eliminates formation and propagation of rigid zones because all points of the structure are brought to rest at the same time in the terminal phase of the shell motion. The unloading criterion was first formulated by Wierzbicki (1972) for viscoplastic structures, and later modified by Wierzbicki (1974) for rigid, perfectly plastic structures.

Differentiating Eq. (50) with respect to $\bar{t}$ gives

$$\bar{w}_{\bar{t}} = \sum_{n=1}^{\infty} [A_n \lambda_n \cos(\lambda_n \bar{t}) - B_n \lambda_n \sin(\lambda_n \bar{t})] \cos(\lambda_n \bar{x}).$$

(54)

Setting Eq. (54) equal to zero signifies that each mode unloads when

$$A_n \cos(\lambda_n \bar{t}) = B_n \sin(\lambda_n \bar{t})$$ (55)

or at a characteristic time $\bar{t}_n$

$$\tan(\lambda_n \bar{t}_n) = \frac{A_n}{B_n}.$$ (56)

The above unloading criterion satisfies both conditions ($\bar{\varepsilon}_{\bar{t}} = 0$ and $\bar{w}_{\bar{t}} = 0$). A closed-form expression for the final deformation profile is obtained by using trigonometric relations to give

$$\cos(\lambda_n \bar{t}_n) = \frac{1}{\sqrt{\left[\left(\dfrac{A_n}{B_n}\right)^2 + 1\right]}}$$ (57)

and

$$\sin(\lambda_n \bar{t}_n) = \frac{A_n/B_n}{\sqrt{\left[\left(\dfrac{A_n}{B_n}\right)^2 + 1\right]}}.$$ (58)

Substituting these into Eq. (50) gives an expression for the final deformation profile

$$\bar{w}_f = \sum_{n=1}^{\infty} [\sqrt{(A_n^2 + B_n^2)} - B_n]\cos(\lambda_n \bar{x}).$$ (59)

For the parabolic distribution, the above equation reduces to

$$\bar{w}_f = \sum_{n=1}^{\infty} \frac{2 \sin \lambda_n}{\lambda_n^4} [\sqrt{(4\bar{I}^2 + \lambda_n^2)} - \lambda_n] \cos(\lambda_n \bar{x});$$

(60)

for the uniform distribution, we get

$$\bar{w}_f = \sum_{n=1}^{\infty} \frac{2 \sin \lambda_n}{\lambda_n^3} [\sqrt{(\lambda_n^2 \bar{I}^2 + 1)} - 1] \cos(\lambda_n \bar{x}).$$

(61)

The solution with an initial velocity distribution that is parabolic converges more rapidly than that with a uniform distribution. The rate of convergence for the parabolic distribution is of the order $1/\lambda_n^3$ while that for the uniform is only of the order of $1/\lambda_n^2$. Simple closed-form expressions for very large impulses may be derived for the series solutions in Eqs. (60) and (61).

Approximation Solutions

Previous analysis shows that a one-term approximation for the central deflection of the shell is within 5% of an eigenfunction solution if $\bar{I} > 1$. (The eigenfunction solution was set to be within a convergence tolerance of 10^{-6}, see Liao, 1993.) Assuming a one-term approximation, we get $\lambda_1 = \pi/2$ and

$$\bar{w}_f = \frac{16}{\pi^4} [\sqrt{(16\bar{I}^2 + \pi^2)} - \pi] \cos\left(\frac{\pi \bar{x}}{2}\right).$$ (62)

The corresponding closed-form expression for the final central deflection is

$$\bar{\delta}_f = \frac{16}{\pi^3} [\sqrt{(16\bar{I}^2/\pi^2 + 1)} - 1], \quad \text{for } \bar{I} > 1.$$ (63)

The series solution in Eq. (61) does not converge as rapidly as that for a parabolically distributed impulse. However, for very large impulses, the term $\sqrt{(\lambda_n^2 \bar{I}^2 + 1)} - 1 \rightarrow \lambda_n \bar{I}$, and Eq. (61) may be rewritten as

$$\bar{w}_f = \bar{I} \sum_{n=1}^{\infty} \frac{2 \sin \lambda_n}{\lambda_n^2} \cos(\lambda_n \bar{x}).$$ (64)

When $\bar{I} > 10$, an approximation to the 50-term series solution in Eq. (64) is

$$\bar{w}_f = 0.742\bar{I}(1 - \bar{x}^2)^{0.7}$$ (65)

and the central deflection is

$$\bar{\delta}_f = 0.742\bar{I}, \quad \text{for } \bar{I} > 10.$$ (66)

It is interesting to note that when the above expression is rewritten in unnormalized quantities, the solution for δ_f is independent $\bar{q}$.

SUMMARY OF DYNA 3D RESULTS

Moussouros and Koenig (1994) have produced DYNA 3D solutions for the impulsively loaded 6061-T6 aluminum shell using the Belytschko–Tsai 5 degree-of-freedom elements with no in-plane torsional components.

The shell geometry was assumed to be a perfectly circular cylinder loaded with an asymmetric radial impulsive load. The $\sigma - \varepsilon$ relationship of 6061-T6 Al material was assumed to be bilinear, i.e., linear elastic, linear strain hardening with the following material properties:

1. $E = 10.8(10^6)$ psi, Young's modulus
2. $\sigma_y = 41,600$ psi, yield strength
3. $E_p = 161,000$ psi, linear strain-hardening modulus
4. $\rho = 2.6(10^{-4})$ lb m/in.^{3}, density.

The bilinear approximation for the $\sigma - \varepsilon$ curve is an idealization of the actual $\sigma - \varepsilon$. For ductile materials, the plastic modulus decreases with increasing strain and the material fractures at a finite value of strain. The plastic strain was extended to 80% (corresponding to a stress of 170,400 psi), even though the shell would fracture before attaining a strain at this value. No fracture criterion was introduced in the numerical simulation because the sole purpose of the numerical exercise was to test the rigid-plastic prediction of the large plastic deformation of the shell.

Several test cases were examined and these are summarized in Table 1. In all cases the peak velocity was 9,670 in./s, except for the first test case where it was set to be 50% higher than the rest, i.e., $V_o = 14,505$ in./s. The first test case has a parabolically distributed impulse and setting the peak velocity at 14,505 in./s results in the same "total" impulse (area under the mass times velocity curve) for Tests 1 and 4.

COMPARISON BETWEEN ANALYTICAL AND DYNA 3D SOLUTIONS

Equivalent functions $\bar{m}$, $\bar{N}$, and $\bar{q}$ depend on the mode of plastic collapse of the ring. Cline and Jahsman (1967) found that a ring subjected to a cosine impulse distribution over its upper half collapses in two stages: a "short-time response," when the plastic work dissipated is predominantly due to membrane compression, and a "long-time response," when the plastic work dissipated is predominantly due to bending at plastic hinges. As shown in Fig. 2, the ring is a membrane mode of plastic collapse during the short-time response and a bending mode during the long-time response. The transition from one mode to the other and/or the interaction of both modes were not addressed by Cline and Jahsman, and will be a topic for future research.

For the particular load cases considered in the DYNA 3D analysis, the ring collapses in the membrane mode. A flow stress of $\sigma_o = 45,000$ psi is used in evaluating equivalent functions for the 6061-T6 aluminum shell in Appendix A. The corresponding values of the equivalent functions are

1. $\bar{m} = 6.1(10)^{-4}$ lb m/in., equivalent mass
2. $\bar{N} = 106,030$ lb, equivalent tensile force
3. $\bar{q} = 22,500$ lb/in., equivalent ring crushing resistance.

The permanent centerline deflection of the shell for all five numerical test cases are compared to the rigid-plastic approximations of them in Table 2. In all cases the analytical predictions are within 25% of numerical results. Test 1 involving a parabolic load distribution of $V_o = 14,505$ in./s has a much higher deformation than Test 4, involving a uniform load distribution with the same total initial impulse. This was expected because the parabolic load is greatest at the centerline.

Table 1. Description of Numerical Test Cases

Test	Radius R (in.)	Thickness h (in.)	Half-Length L (in.)	D/h	Axial Load Distribution	Impulse Velocity V_o (in./s)
1	6	0.25	2	48	Parabolic	14,505
2	6	0.25	2	48	Parabolic	9,670
3	6	0.25	4	48	Parabolic	9,670
4	6	0.25	2	48	Uniform	9,670
5	6	0.25	4	48	Uniform	9,670

Membrane Mode
(short-time response)

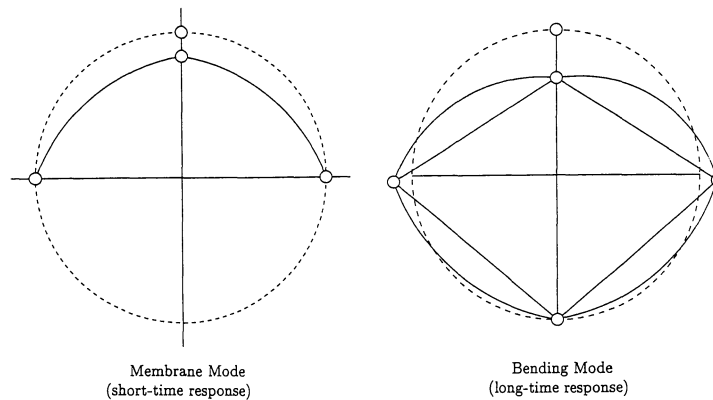Bending Mode
(long-time response)

FIGURE 2 Plastic collapse of ring in membrane and bending modes.

Calculations show that, for the given diameter to thickness ratio of the shells considered by DYNA 3D, the equivalent ring crushing resistance, i.e., the equivalent plastic foundation force, in a bending mode is 2 orders of magnitude less than that in a membrane mode. An equivalent ring crushing resistance that assumes both membrane and bending modes would therefore be lower than one calculated with only a membrane mode. This explains why analytical predictions were less than the numerical solutions. In calculating equivalent functions, the bending mode during the long-time response of the shell was ignored, and the resulting foundation force is stiffer. A plastic collapse ring model that assumes both membrane and bending modes should bring analytical predictions closer to the numerical results.

The analytical predictions of the transient and final deflection profiles of the shell in the circumferential and longitudinal direction for Test 4 are compared to the numerical predictions in Figs. 3 and 4. The shell undergoes about 10% circumferential compression on the upper half of its circumference so that a considerable amount of plastic work is dissipated during hoop compression. The analytical predictions of the transient deflections

in the circumferential and longitudinal directions at $t = 46.9 \mu s$ and $92.8 \mu s$, respectively, are within 5% of the DYNA 3D predictions. To compare analytical and numerical predictions of the final deformed profiles, it was assumed that the elastic vibrations in the DYNA 3D analysis attenuated completely at $t = 138.6 \mu s$. The rigid-plastic approximation for the final deformation is within 25% of the DYNA 3D prediction of the shell deformation at $t = 138.6 \mu s$.

A comparison between the rigid-plastic approximation and the numerical solution of the transient response of the maximum centerline deflection for Tests 2 and 4 are also shown in Fig. 5. Plastic unloading in the rigid-plastic approximation occurs near the first overshoot of the elastic shell vibrations. The predicted plastic response times of the shell are within 10% of the numerical predictions (measured by the time at the first overshoot of the elastic shell vibrations).

CONCLUDING REMARKS

A theoretical approach for predicting the plastic deformation of a cylindrical shell subject to asymmetric dynamic loads was developed and com-

Table 2. Comparison of DYNA 3D and Analytical Results

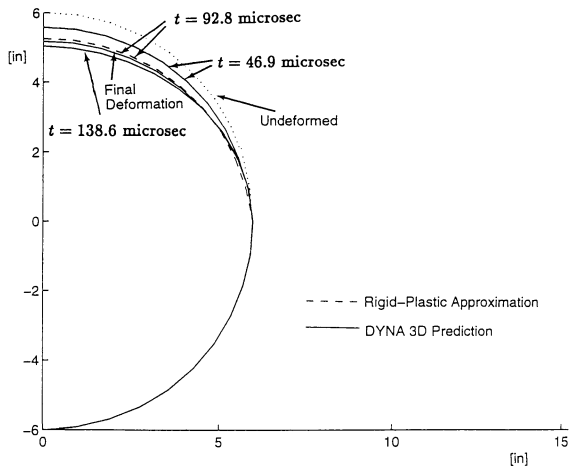| Test	$\bar{I} = V_o\overline{N}/cL\bar{q}$	Analytical $\delta_f =$ $\delta_f L^2 \bar{q}/\overline{N}$ (in.)	Numerical δ_f (in.)	% Underprediction
1	2.61	1.08	1.20	−10
2	1.74	0.62	0.77	−19
3	0.87	0.86	1.14	−25
4	1.74	0.75	0.97	−23
5	0.87	1.06	1.30	−18

FIGURE 3 Circumferential deflection profile at $x = 0$ of the shell. Test 4: uniform velocity = 9670 in./s, $2R = 12$ in., $2L = 4$ in., $h = 0.25$ in.
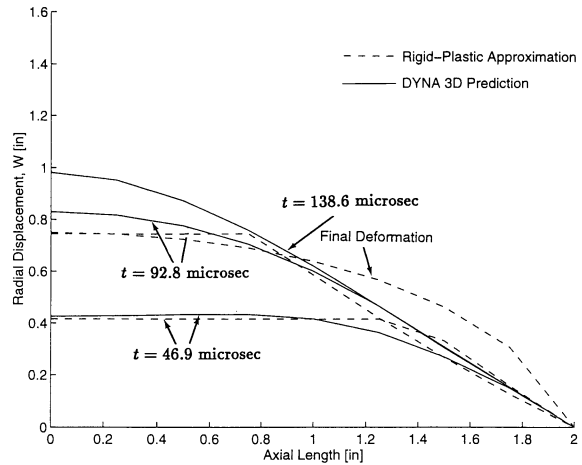

FIGURE 4 Transient and final deflection profile of the leading generator of the shell. Test 4: uniform velocity = 9670 in./s, $2R = 12$ in., $2L = 4$ in., $h = 0.25$ in.

pared to numerical results from DYNA 3D. The plastic deformation of the shell was found by solving for the transverse deflections of a rigid-plastic beam/string-on-foundation. As an example, the deformation of a cylindrical shell subject to impulsive loading was predicted by finding the solution of the transient and final deformations of a string-on-foundation. Equivalent functions for the string-on-foundation were evaluated using a membrane mode plastic collapse mechanism for the shell. The analytical predictions of the centerline shell deflection underpredicted the DYNA 3D results by 25%. The discrepancy between the analytical and numerical solutions was attributed to neglecting the bending mode or long-time response of the shell. A plastic collapse ring model that assumes both membrane and bending phases would result in a reduction of the equivalent crushing resistance of the shell and should increase analytical predictions, bringing them closer to the numerical results. Analyzing plastic collapse of a ring in combined membrane and bending modes will be the subject of future research.

APPENDIX A: EQUIVALENT FUNCTIONS

Equivalent functions for the impulsively loaded shell are calculated for the membrane mode plastic collapse mechanism shown in Fig. 2.

Following Cline and Jahsman (1967), the deformation in the upper half of the shell circumference

is described by a cosine distribution

$$w(\theta) = w_o \cos \theta. \tag{A.1}$$

Velocity and accelerations fields are similarly described by cosine distributions, $\dot{w}(\theta) = \dot{w}_o \cos \theta$ and $\ddot{w}(\theta) = \ddot{w}_o \cos \theta$.

To evaluate the fully plastic bending moments and tensile forces, assume a limited interaction yield curve

$$|M_{\theta\theta}| = M_{\text{pl}}, \quad |N_{\theta\theta}| = N_{\text{pl}}, \quad |N_{xx}| = N_{\text{pl}}, \tag{A.2}$$
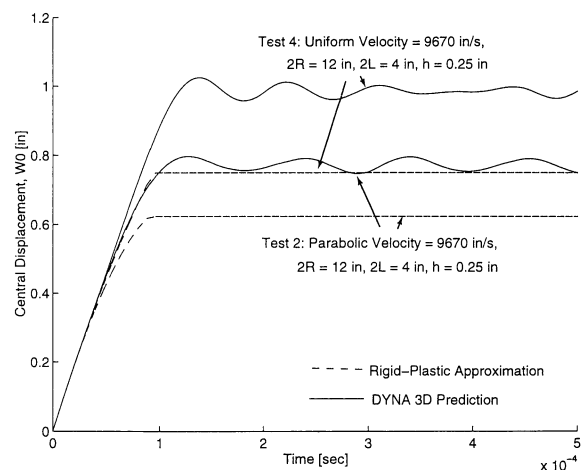

FIGURE 5 Transient centerline deflection of the leading generator of the shell for shells. Test 2: parabolic velocity = 9670 in./s, $2R = 12$ in., $2L = 4$ in., $h = 0.25$ in. Test 4: uniform velocity = 9670 in./s, $2R = 12$ in., $2L = 4$ in., $h = 0.25$ in.

where $M_{pl} = \sigma_o h^2/4$ is the fully plastic bending moment per unit length and $N_{pl} = \sigma_o h$ is the fully plastic axial force per unit length.

With the above distribution, Eq. (A.1), and value for N_{pl}, the equivalent mass and tensile force, defined by Eqs. (11) and (14), are

$$\bar{m} = 2Rm \int_0^\pi \cos^2\theta \, d\theta = \pi R\rho h/2$$

equivalent mass per unit length and

$$\bar{N} = 2RN_{pl} \int_0^\pi \cos^2\theta \, d\theta = \pi R\sigma_o h/2$$

equivalent tensile force.

The equivalent ring resistance depends on the plastic work dissipated in membrane compression

$$\bar{q}(x, t) = \frac{2R}{\dot{w}_o} \int_0^\pi N_{\theta\theta}\dot{\varepsilon}_{\theta\theta} \, d\theta. \qquad (A.3)$$

Neglecting tangential component and higher order terms, one can approximate the hoop strain rate as

$$\dot{\varepsilon}_{\theta\theta} = \begin{cases} \dfrac{\dot{w}_o}{R}\cos\theta, & \text{for } |\theta| < \pi/2 \\ 0, & \text{otherwise.} \end{cases} \qquad (A.4)$$

Substituting Eq. (A.4) into Eq. (A.3) and integrating give

$$\bar{q} = 2\sigma_o h \int_0^{\pi/2} \cos\theta \, d\theta = 2\sigma_o h. \qquad (A.5)$$

REFERENCES

Brush, D. O., and Almroth, B. O., 1975, "Strain Localization and Fracture in Metal Sheets and Thin-Walled Structures," in *Buckling of Bars, Plates, and Shells*, McGraw-Hill, New York.

Cline, G. B., and Jahsman, W. E., 1967, "Response of a Rigid-Plastic Ring to Impulsive Loading," *Journal of Applied Mechanics*, Vol. 89, pp. 329–336.

Greenspon, J. E., 1970, "Theoretical Calculation of Iso-Damage Characteristics," Ballistic Research Laboratory, J. G. Eng. Res Assoc., Technical Report No. 10, February.

Haythornwaite, R. M., 1961, "Mode Change During the Plastic Collapse of Beams and Plates," in *Developments in Mechanics, Proceedings of the 7th Midwestern Mechanics Conference*, Vol. 1, J. E. Lay and L. E. Malvern, pp. 203–215.

Jiang, J., and Olson, M. D., 1991, "Nonlinear Dynamic Analysis of Blast Loaded Cylindrical Shell Structures," *Computers & Structures*, Vol. 41, No. 1, pp. 41–52.

Jones, N., 1971, "A Theoretical Study of the Dynamic Plastic Behavior of Beams and Plates with Finite Deflections," *International Journal of Solids and Structures*, Vol. 7, pp. 1007–1029.

Liao, S.-W., 1993, "Dynamic Failure of Cylindrical Shells," Final report for the Master of Science degree program in the Naval Architecture and Offshore Engineering Department, University of California, Berkeley.

Martin, J. B., and Symonds, P. S., 1966, "Mode Approximation for Impulsively Loaded Rigid-Plastic Structures," *Journal of the Engineering Mechanics Division, Proceedings ASCE*, Vol. 92, No. EM5, pp. 43–66.

Moussouros, M., and Hoo Fatt, M. S., 1995, "Effect of Shear on Plastic Denting of Cylinders," *International Journal of Mechanical Sciences*, Vol. 37, No. 4, pp. 355–371.

Moussouros, M., and Koenig, J., 1994, "Validation of Rigid-Plastic Model for the Dynamic Response of a 6061-T6 Aluminum Shell Subject to Impulsive Loading Using DYNA 3D," Personal Communications, NSWC, White Oak.

Reid, S. R., 1978, "Influence of Geometrical Parameters on the Mode of Collapse of a "Pinched" Rigid-Plastic Cylindrical Shell," *International Journal of Solids and Structures*, Vol. 14, pp. 1027–1043.

Stricklin, J. A., Haisler, W. E., and von Riesemann, W. A., 1974, "Large Deflection Elastic-Plastic Dynamic Response of Stiffened Shells of Revolution," *Journal of Pressure Vessel Technology*, May, pp. 87–95.

Suliciu, M. M., Suliciu, I., Wierzbicki, T., and Hoo Fatt, M. S., 1996, "Transient Response of an Impulsively Loaded Plastic String on a Plastic Foundation," *Quarterly Applied Mathematics*, to appear.

Underwood, P., 1972, "Transient Response of Inelastic Shells of Revolution," *Computers & Structures*, Vol. 2, pp. 975–989.

Vaziri, R., Olson, M. D., and Anderson, D. L., 1987, "Dynamic Response of Axially Constrained Plastic Beams to Blast Loads," *International Journal of Solids and Structures*, Vol. 23, No. 1, pp. 153–174.

Wierzbicki, T., 1972, "An Approximate Linear Theory of Thin Viscoplastic Shells," *Archives of Mechanics*, Vol. 24, No. 5–6, pp. 941–953.

Wierzbicki, T., 1974, "Application of an Eigenfunction Expansion Method in Plasticity," *Journal of Applied Mechanics,* Vol. 41, No. 2, pp. 448–452.

Wierzbicki, T. and Suh, M. S., 1988, "Indentation of Tubes Under Combined Loading," *International Journal of Mechanical Science,* Vol. 30, No. 3/4, pp. 229–248.

Witmer, E. A., Herrmann, W., Leech, J. W., and Pian,

T. H. H., 1960, "Responses of Plates and Shells to Intense External Loads of Short Duration," Massachusetts Institute of Technology Technical Report WADD TR 60-433, April.

Yu, T. X., and Stronge, W., 1990, "Large Deflection of a Rigid-Plastic Beam-on-Foundation from Impact," *International Journal of Impact Engineering,* Vol. 9, pp. 115–126.